J. Appl. Comput. Mech., 6(3) (2020) 480-492
DOI: 10.22055/JACM.2019.30188.1696

ISSN: 2383-4536
jacm.scu.ac.ir

M&MoCS

Shahid Chamran University of Ahvaz

Journal of Applied and Computational Mechanics

Research Paper

Emotional Learning Based Intelligent Controller for MIMO Peripheral Milling Process

Arash Bahari Kordabad[1], **Mehrdad Boroushaki**[2]

[1] Department of Mechanical Engineering, Sharif University of Technology
Azadi Ave, Tehran, 13547-87653, Iran, Email: Arashbahari20@gmail.com

[2] Department of Energy Engineering, Sharif University of Technology
Azadi Ave, Tehran, 14565-114, Iran, Email: boroushaki@sharif.edu

Received July 03 2019; Revised August 15 2019; Accepted for publication August 15 2019.
Corresponding author: A. Bahari Kordabad (Arashbahari20@gmail.com)

Abstract. During the milling process, one of the most important factors in reducing tool life expectancy and quality of workpiece is the chattering phenomenon due to self-excitation. The milling process is considered as a MIMO strongly coupled nonlinear plant with time delay terms in cutting forces. We stabilize the plant using two independent Emotional Learning-based Intelligent Controller (ELIC) in parallel. Control inputs are considered as forces Ux and Uy in two directions x and y, which are applied by the piezoelectrics. The ELIC consists of three elements; Critic, TSK controller and the learning element. The results of the ELIC have been compared with a Sliding Mode Controller (SMC). The simulation for the nominal plant shows better performance of the ELIC in IAE and ITSE values at least 86% in the x-direction and 79% in the y-direction. Similar simulation for an uncertain plant also shows an improvement of at least 89% in the x-direction and 97% in the y-direction.

Keywords: Emotional learning, Intelligent control, Peripheral milling, nonlinear MIMO, Time-delay, Sliding mode.

1. Introduction

The machining process and, in particular, the milling is one of the most important parts in manufacturing industry field. The importance of this field has been enlarged with the advancement of technology and the development of new CNC, CAD/CAM machines. In general, the milling process is divided into three types of peripheral, face milling and end-milling [1]. In peripheral milling, the surface of the workpiece is created by the teeth based on the shearing tool environment, and the tool axis is generally in the parallel plane with the machined surface of the workpiece. In the face milling, the surface of the workpiece is created by the teeth based on the environment and the floor of the tool, and the spindle axis is perpendicular to the machined surface. The end milling is a combination of peripheral and plate milling. Fig. 1 shows the different types of the milling process.

In recent years, with the advancement of machining industries, expectations have been raised to meet the manufacturing requirements such as improving surface fineness, low durability, high raw material yields, high lifetime and high resistance of tools, and even lessening of the annoying noise of machining. Most of these requirements can be analyzed and realized by studying the complex dynamics of the machining process.

Tool vibrations consist of three types of transient, forced, and self-excitation, the most important of which is the self-excitation vibration. The milling process is a nonlinear system, due to the stiffness of the structure and the cutting forces. Nonlinear modeling of this process would reveal some nonlinear properties such as bifurcation, limit cycles, and chaos phenomena, while linear modeling would not.

Published online: September 15 2019

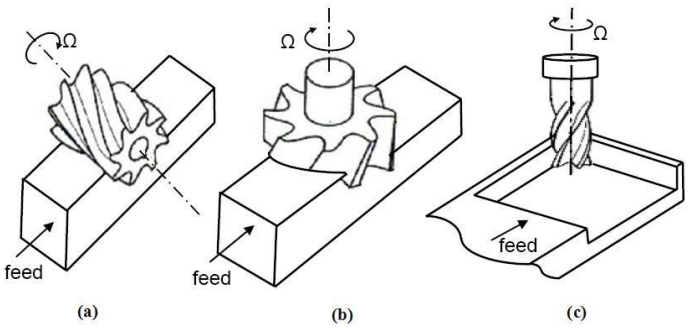

Fig. 1. Different types of the milling process. a) Peripheral b) Face and c) End milling.

The researches on the vibration of the milling process have been begun with the works in Tobias and Fishwick [2] and Tlusty [3]. They introduced two main factors of self-excitation named regenerative chatter and mode coupling. Henceforth, other researches considered the modeling and analyzing of the process [4]. Moradi developed the nonlinear equations of the milling process considering the structural and cutting force nonlinearities [5] and bifurcation analysis of the process [6].

There can be found several passive and active control strategies in the reduction of the vibration in the machining process. Optimal passive vibration control [7], tunable vibration absorber [8], design and implementation of tuned viscoelastic dampers [9], spindle speed variation and adaptive force regulation [10], and chatter prevention by acoustic signal feedback [11] are among the passive approaches. Model reference adaptive control [12], robust strategy [13] and reducing the amplitude of vibration of the milling process via a robust optimal control approach [14] have been used as the active vibration control.

In the field of intelligent and fuzzy control, studies have been carried out since the 1990s. It was shown that a fuzzy-neural controller could stabilize complex manufacturing processes [15]. The results show that the fuzzy-neuro approach can give a robust and accurate method of controlling complex processes without comprehensive models or information about the process. In the work [16] two types of the intelligent adaptive controller based on optimization for the milling process was proposed. Moreover, Janabi-Sharifi [17] presented a fuzzy-neural system for looper tension control in rolling mills. Zuperl, Cus [18] introduced a fuzzy control strategy to control the adaptive force of the high-speed end milling. They showed robustness and global stability of this approach. Thellaputta, Raju [19] proposed an adaptive neuro-fuzzy approach for predicting cutting forces with rotary tools in the milling process. Furthermore, intelligent active fixtures has been used to stabilize the process by generating counteracting oscillations and also active chatter control in milling [20].

The milling process is a MIMO strongly coupled nonlinear model due to structure stiffness and third order polynomials for the cutting forces with time delay. Controlling of MIMO nonlinear process with time delay has always been a challenging issue [21]. Huang proposed a MIMO model with linear structure stiffness [13]. Moradi, Movahhedy [22] used a SISO model with a robust control strategy for suppression of the regenerative chatter in the turning process.

By studying the stability lobes can be realized that increasing the cutting axial depth causes system instability [4]. The high-speed milling process has an important role in the manufacturing industry. Several studies have been focused on the modeling and analysis of high-speed milling for prediction of regenerative chatter [23]. High-speed milling process can provide a big number of ready workpieces in a short time [24].

In this paper, a high-speed milling process with a large axial depth of cut is considered. We have proposed a new intelligent controller named, Emotional Learning-based Intelligent Controller (ELIC) to reduce the amplitude of the vibrations in the milling process. ELIC is a novel adaptive and robust strategy for controlling nonlinear systems, which has been already used for load-frequency control [25] and steam generator water level [26]. Also, Khadem, Behzadipour [27] illustrated that the implementation of this type of controller is simply practical for force control of a robotic laparoscopic instrument.

We have considered the milling process as a MIMO strongly coupled nonlinear plant with time delay terms and two inputs as forces Ux and Uy which provided via the piezoelectrics and two outputs as displacements x and y. The model equations are based on the model of Moradi, Vossoughi [14], while the results have been compared with the Sliding Mode Controller (SMC). The simulation results show the simple structure of the ELIC compares to the classic controller.

2. Dynamic Modeling of the Milling System

Tool chatter in the milling process is due to the two important phenomena, regeneration of waves and the mode coupling [2]. Regeneration of waves is covered by the most milling process models. Fig. 2 shows the 2-dimensional dynamic of peripheral milling. The immersion angle for flute j, (φ_j), is a function of immersion angle (φ) as follows [14]:

$$\phi_j(z) = \phi + j\phi_p - (2z/D)\tan\beta; \qquad j = 0,1,...,N-1 \tag{1}$$

where, ϕ_p is the cutter pitch angle and it would be equal to $2\pi/N$, and N is the number of cutter teeth, z is axial depth,

β is helix angle and D is the diameter of the cutter. To increase the accuracy of the model, the cutting forces ($F_{t,j}$ and $F_{r,j}$) are expressed as a third-order polynomial of the cut chip thickness $h(\phi_j)$ as follows:

$$\begin{aligned} dF_{t,j}(\phi,z) &= [\zeta_1 h_j^3(\phi_j(z)) + \zeta_2 h_j^2(\phi_j(z)) + \zeta_3 h_j(\phi_j(z)) + \zeta_4]dz \\ dF_{r,j}(\phi,z) &= [\eta_1 h_j^3(\phi_j(z)) + \eta_2 h_j^2(\phi_j(z)) + \eta_3 h_j(\phi_j(z)) + \eta_4]dz \end{aligned} \tag{2}$$

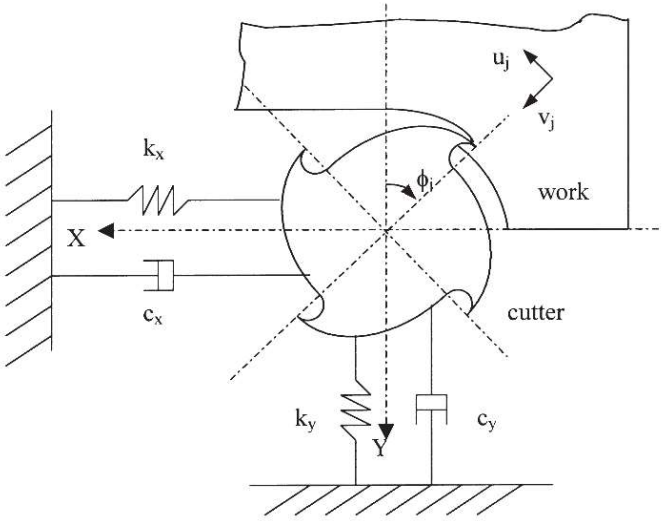

Fig. 2. The 2-dimensional dynamic of peripheral milling.

where $\zeta_i, \eta_i \; i = 1,\ldots,4$ are cutting force coefficients that can be obtained from the experiment. These coefficients are directly related to the axial depth of cut a_c. The dynamic chip thickness in regenerative chatter $h(\phi_j)$ can be expressed as:

$$h(\phi_j) = [\Delta x \sin\phi_j + \Delta y \cos\phi_j] g(\phi_j) \tag{3}$$

where

$$\Delta x = x(t) - x(t-\tau); \quad \Delta y = y(t) - y(t-\tau); \quad \tau = \frac{2\pi}{N\Omega} \tag{4}$$

x and y are displacements (system outputs), τ is the time delay in[s], Ω is spindle speed in [rad/s], and the function $g(\phi_j)$ is a step function which determines the effective range of the chip thickness function. Considering the start immersion angle ϕ_{st} and the exit immersion angle ϕ_{ex}, we have:

$$g(\phi_j) = \begin{cases} 1 & \phi_{st} < \phi_j < \phi_{ex} \\ 0 & \phi_{st} > \phi_j \; or \; \phi_{ex} < \phi_j \end{cases} \tag{5}$$

The dynamics of the 2-D peripheral milling process in modal form can be expressed as follows:

$$\begin{aligned} \ddot{x} + 2(\hat{\mu}_x + \hat{\mu}_{xp})\dot{x} + \omega_x^2 x + \hat{\delta}_1 x^2 + \hat{\delta}_2 x^3 &= \hat{F}_x(\Delta x, \Delta y) \\ \ddot{y} + 2(\hat{\mu}_y + \hat{\mu}_{yp})\dot{y} + \omega_y^2 y + \hat{\lambda}_1 y^2 + \hat{\lambda}_2 y^3 &= \hat{F}_y(\Delta x, \Delta y) \end{aligned} \tag{6}$$

where the following relationships exist between the parameters:

$$\begin{aligned} &\hat{\mu}_i = \zeta_i \omega_i \;,\; \zeta_i = \frac{c_i}{2\sqrt{k_i m_i}} \;,\; \omega_i^2 = \frac{k_i}{m_i} \;,\; \hat{F}_i = \frac{F_i}{m_i} \;,\; \hat{\delta}_j = \frac{\delta_j}{m_x} \;, \\ &\hat{\lambda}_j = \frac{\lambda_j}{m_y}, \hat{\mu}_{ip} = \zeta_{ip}\omega_i \;,\; \zeta_{ip} = \frac{\Gamma_i}{2\Omega\sqrt{k_i m_i}} \;,\; i = x, y \;\; j = 1,2 \end{aligned} \tag{7}$$

These parameter values are presented in Table 1. By projecting Eq. (2) on the x and y directions and using the first term of Fourier series expansion the closed-form expressions for nonlinear cutting forces are described as follows [14]:

$$F_x = -\frac{N}{2\pi}\left\{\alpha_1\Delta x^3 + \beta_1\Delta y^3 + \alpha_2\Delta x^2 + \beta_2\Delta y^2 + \alpha_3\Delta x + \beta_3\Delta y + 3\gamma_1\Delta x^2\Delta y + 3\gamma_2\Delta x\Delta y^2 + 2\gamma_3\Delta x\Delta y + \gamma_4\right\}$$
$$F_y = \frac{N}{2\pi}\left\{\alpha_1'\Delta x^3 + \beta_1'\Delta y^3 + \alpha_2'\Delta x^2 + \beta_2'\Delta y^2 + \alpha_3'\Delta x + \beta_3'\Delta y + 3\gamma_1'\Delta x^2\Delta y + 3\gamma_2'\Delta x\Delta y^2 + 2\gamma_3'\Delta x\Delta y + \gamma_4'\right\} \tag{8}$$

For half immersion up-milling with $\phi_{st} = 0$ and $\phi_{ex} = \pi/2$, the forces coefficients $\alpha_i, \beta_i, \alpha_i', \beta_i', \gamma_j, \gamma_j'$, ($i = 1,2,3$, $j = 1,...,4$) $j = 1,...,4$) are calculated as Eq. (9).

$$\begin{aligned}
&\alpha_1 = \frac{1}{4}[\xi_1 + \frac{3}{4}\pi\eta_1], \quad \beta_1 = \frac{1}{4}[\eta_1 + \frac{3}{4}\pi\xi_1], \quad \alpha_2 = \frac{1}{3}[\xi_2 + 2\eta_2], \quad \beta_2 = \frac{1}{3}[\eta_2 + 2\xi_2], \quad \alpha_3 = \frac{1}{2}[\xi_3 + \frac{1}{2}\pi\eta_3]\\
&\beta_3 = \frac{1}{2}[\eta_3 + \frac{1}{2}\pi\xi_3], \quad \gamma_1 = \frac{1}{4}[\eta_1 + \frac{1}{4}\pi\xi_1], \quad \gamma_2 = \frac{1}{4}[\xi_1 + \frac{1}{4}\pi\eta_1], \quad \gamma_3 = \frac{1}{3}[\xi_2 + \eta_2], \quad \gamma_4 = \xi_4 + \eta_4\\
&\alpha_1' = \frac{1}{4}[-\eta_1 + \frac{3}{4}\pi\xi_1], \quad \beta_1' = \frac{1}{4}[\xi_1 - \frac{3}{4}\pi\eta_1], \quad \alpha_2' = \frac{1}{3}[-\eta_2 + 2\xi_2], \quad \beta_2' = \frac{1}{3}[\xi_2 - 2\eta_2], \quad \alpha_3' = \frac{1}{2}[-\eta_3 + \frac{1}{2}\pi\xi_3]\\
&\beta_3' = \frac{1}{2}[\xi_3 - \frac{1}{2}\pi\eta_3], \quad \gamma_1' = \frac{1}{4}[\xi_1 - \frac{1}{4}\pi\eta_1], \quad \gamma_2' = \frac{1}{4}[-\eta_1 + \frac{1}{4}\pi\xi_1], \quad \gamma_3' = \frac{1}{3}[\xi_2 - \eta_2], \quad \gamma_4' = \xi_4 - \eta_4
\end{aligned} \tag{9}$$

Table 1. Values of model parameters

Parameter	Characteristic	Value	Unit	Parameter	Characteristic	Value	Unit
k_x	Stiffness	7.2×10^6	N/m	ζ_x	Damping ratio	0.05	-
k_y		6.48×10^7		ζ_y		0.06	
m_x	Mass	20	kg	ω_x	Natural frequency	600	rad/s
m_y		20		ω_y		1800	
c_x	Damping	1200	$N.s/m$	$\hat{\delta}_1$	Nonlinear stiffness	3.5×10^8	$N/kg.m^2$
c_y		4300		$\hat{\delta}_2$		4×10^{11}	$N/kg.m^3$
N	Cutter teeth number	4	-	$\hat{\lambda}_1$		4×10^8	$N/kg.m^2$
a_c	Cutting axial depth	22	mm				
Ω	Spindle speed	10000	rpm	$\hat{\lambda}_2$		4.5×10^{11}	$N/kg.m^3$
Γ_x	Contact force coefficient	8.4×10^4	N/m	(Cutting forces coefficients for a_c=2.5 mm)			
Γ_y		9.6×10^4		ξ_1=6765 N/mm^3,ξ_2=-4910 N/mm^2,ξ_3=2840 N/mm,ξ_4=134 N			
β	Helix angle	0	rad	η_1=12740 N/mm^3,η_2=-7452 N/mm^2,η_3=1674 N/mm,η_4=246 N			

Finally, regarding the above equations, the milling process can be modeled as a MIMO plant with two inputs as forces U_x and U_y, and two outputs displacements x and y. The modal form of the conclusive equation can be expressed as follows:

$$\begin{aligned}
\ddot{x} + 2(\hat{\mu}_x + \hat{\mu}_{xp})\dot{x} + \omega_x^2 x + \hat{\delta}_1 x^2 + \hat{\delta}_2 x^3 &= \hat{F}_x(\Delta x, \Delta y) + u_x\\
\ddot{y} + 2(\hat{\mu}_y + \hat{\mu}_{yp})\dot{y} + \omega_y^2 y + \hat{\lambda}_1 y^2 + \hat{\lambda}_2 y^3 &= \hat{F}_y(\Delta x, \Delta y) + u_y
\end{aligned} \tag{10}$$

where

$$u_i = U_i/m_i \quad , \quad i = x, y \tag{11}$$

Since in Eqs. (8) and (10) the two outputs x and y have appeared in both equations with the order of three, thus one output is affected by the other output. This type of systems is MIMO strongly coupled plant.

3. Emotional Learning-based Intelligent Control (ELIC)

Decision-making skills in human as an intelligent biological system is based on cognition and emotion. In the human's action, the emotional elements such as stress, excitement or satisfaction have an important role. Human beings always try to decrease their stress concerning the environment to achieve a specific goal [28].

Recently, many studies have been carried out for the computational modeling of human emotional learning. In this paper, we used cognitive restatement of reinforcement learning [29]. In this approach, there is a critic or supervisor element whose task is to evaluate the controller. The critic produces stress (emotional) signal which should be minimized by updating the controller weights.

Emotional learning is very similar to reinforcement learning, but the critical difference is in the supervisor's evaluating signal r. In classical reinforcement learning, the supervisor's signal is a binary signal based on failure/success, i.e. r =+1 for failure and r = 0 for success [30]. However, in the ELIC approach, the stress signal r is a continuous signal and can be

any arbitrary values in [-1, +1] interval. As the stress signal is closer to zero, the behavior of the system is more favorable. An emotional learning-based intelligent controller (ELIC) consists of three major components. a) The critic evaluates the behavior of the whole system and provides a stress signal. b) The neuro-fuzzy controller that takes the error and its derivative and, based on its weights, produces a control input signal. c) The learning element, which is based on an optimization process like steepest descent that updates the weights of the neuro-fuzzy controller. Fig .3 shows the structure of the ELIC and its components.

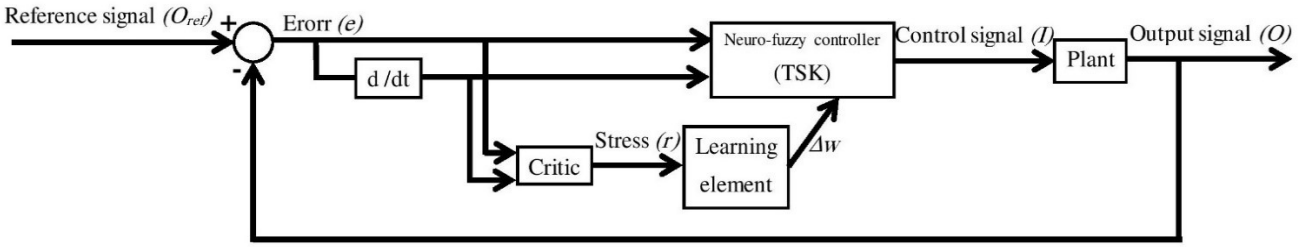

Fig. 3. The structure of ELIC and its components

3.1 Neuro-fuzzy Controller

In general ELIC structure, a Takagi-Sugeno-Kang (TSK) network is used as the neuro-fuzzy controller [31]. The TSK as a fuzzy system is based on the knowledge of IF-THEN rules as follows:

R_i : If (x_1 is F_{i1}) and (x_2 is F_{i2}) and … and (x_n is F_{in}) , Then ($I_i=g_i(X)$), $i=1,2,\ldots,N$

where R_i is the i^{th} rule, N is the total number of rules, $X=[x_1, x_2, \ldots, x_n]$ is the input vector, F_{ij} is the i^{th} linguistic value (j=1,2,…,n), n is the number of inputs, and $I_i=g_i(X)$ is the consequence of the corresponding rule.

As shown in Fig. 4, TSK neural network is formed of 5 layers with two inputs and one output. The first layer consists of fuzzy membership functions that map the inputs data into [-1,1] interval. The second layer is a multiplier, and its outputs are the firing strengths of the rule u_i. Indeed, in this neuro-fuzzy system, we use product-operation for "and" action. The third layer normalizes the firing strengths in IF section of each rule. In the fourth layer, the normalized firing strengths multiply in "then" part of rules. Finally, in the fifth layer, the output is computed as the sum of the weighted average. As Fig. 4 the output of the neural network with two inputs e and de/dt and one output I can be written as:

$$I=\sum_{i=1}^{N}\overline{u}_i\left(a_i e+b_i\dot{e}+c_i\right),\quad \overline{u}_i=u_i\Big/\sum_{i=1}^{N}u_i \tag{12}$$

where $X=[x_1, x_2]=[e, de/dt]$ is the input vector (n=2), $I_i=g_i(X)$ is the consequence section of the i^{th} rule, a_i, b_i and c_i are the weights at fourths layer of the TSK controller that will be regulated by the learning element.

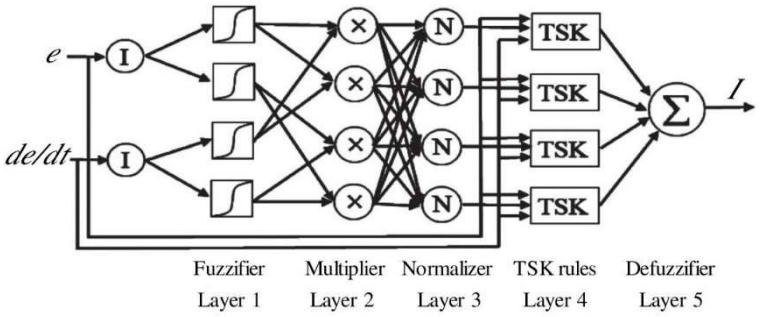

Fig. 4. The structure of the TSK neural network

3.2 Critic

The critic is the main unit used in ELIC and has the task of performing emotional learning control approach. In general, the critic inputs can be system outputs, errors, and its derivatives or any specific parameters of the plant that is required for a correct evaluation of the whole system. The goal in the ELIC is to reduce the absolute value of the critic output stress r. If the system cost function is defined as follows:

$$E=\frac{1}{2}r^2 \tag{13}$$

Then the aim would be to minimize the E over time.

3.3 Learning Element

As it was mentioned in the previous section, the objective of ELIC is always reducing the stress signal r. Using the steepest descent method, TSK weight (w) updating should be in the opposite direction of the gradient E. Thus:

$$\Delta w = -\eta \frac{\partial E}{\partial w} \tag{14}$$

where η is the learning rate. Using the chain rule, it can be written:

$$\Delta w = -\eta \frac{\partial E}{\partial w} . \frac{\partial r}{\partial e} . \frac{\partial e}{\partial O} . \frac{\partial O}{\partial I} . \frac{\partial I}{\partial w} \tag{15}$$

where I is the control action, O is the output and $\partial O / \partial I$ is the Jacobian of the plant. By assuming some assumptions such as substituting the sign of the Jacobian instead of its exact value, one can simplify the learning rule as follows:

$$\Delta w = +\eta r \frac{\partial I}{\partial w} \tag{16}$$

By considering a_i, b_i and c_i as the TSK weights, the updating equations would be as follows:

$$a_{i,new} = a_{i,old} + \eta r e \bar{u}_i \tag{17a}$$

$$b_{i,new} = b_{i,old} + \eta r \dot{e} \bar{u}_i \tag{17b}$$

$$c_{i,new} = c_{i,old} + \eta r \bar{u}_i \tag{17c}$$

4. The Architecture of the Milling Process Controller

The milling process can be modeled as a MIMO plant with two inputs U_x and U_y and two outputs x and y. As Eq. (8) and Eq. (10) show the input outputs are strongly coupled, where the forces in Eq. (8) include the time delay terms. Thus, any proposed controller should consider this level of complexity to control the whole plant.

To overcome this complexity in control engineering, the controller has to consider the detailed nature of the MIMO plant. One of the best advantages of intelligent based control systems such as ELIC is in self-capturing of the system dynamics. The previous studies in this field proof this capability of the ELIC [25].

To capture the coupling of the input outputs and time delays in the milling process, we have proposed a two distinct and parallel ELIC structure in Fig. 5.

The critic can be designed via different structure from a simple PD or a fuzzy system. Considering that the plant is complex nonlinear, it is preferable to consider the critic as a fuzzy system with fuzzifier, defuzzifier, and fuzzy inference engine structure (see Fig. 5). The membership functions and nine fuzzy rules (N=9) of the critic are shown in Fig. 6 and Table 2, where the defuzzifier output is calculated according to the Eq. (18).

$$r^* = \frac{\int r \mu(r) dr}{\int \mu(r) dr} \tag{18}$$

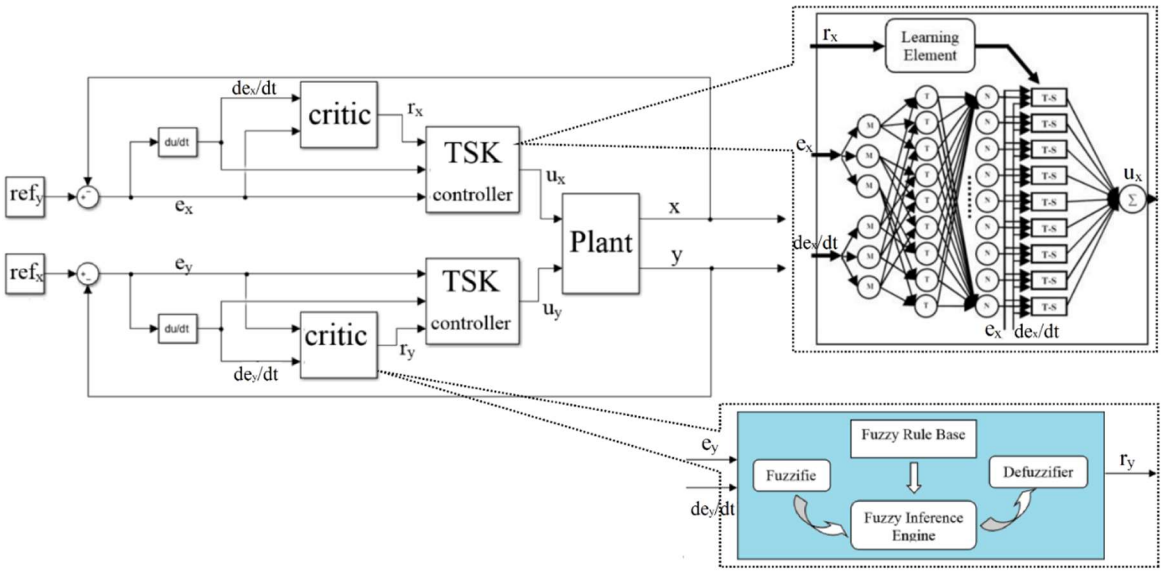

Fig. 5. The structure of two ELICs for controlling a MIMO milling process.

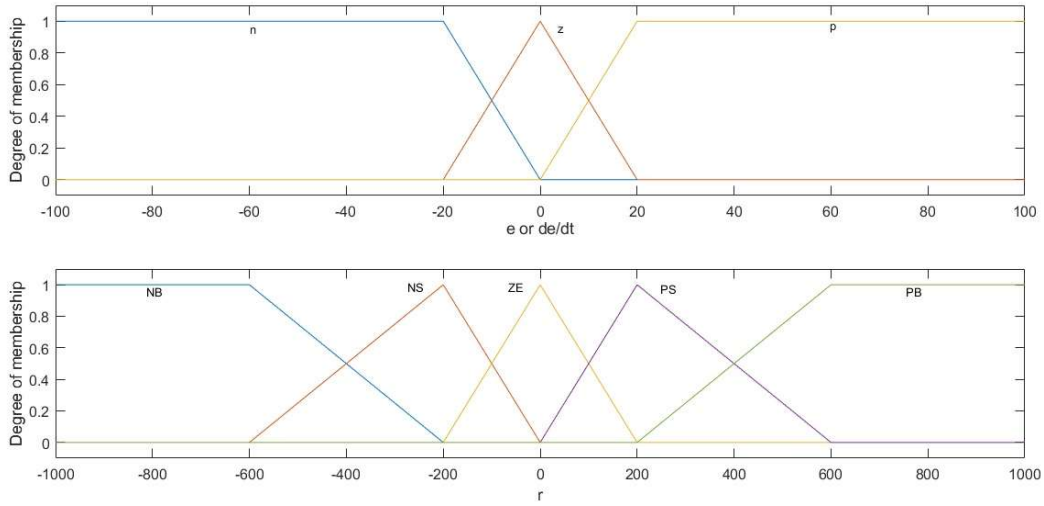

Fig. 6. Fuzzy membership functions of the critic (e and de/dt are inputs, and r is output)

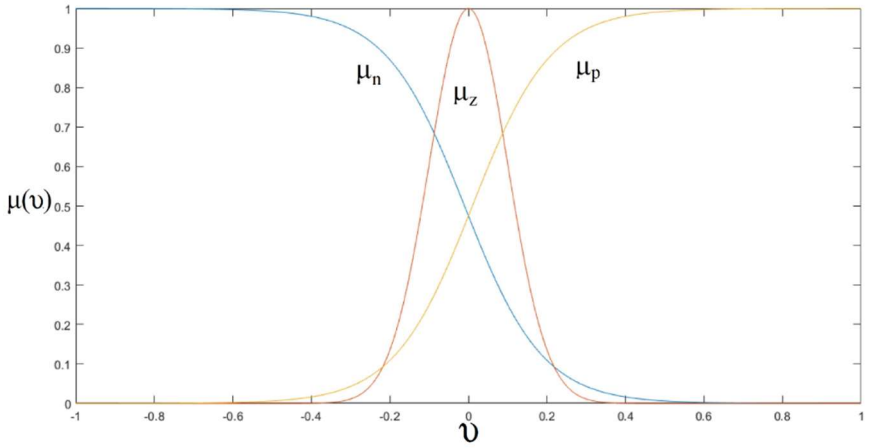

Fig. 7. Fuzzy membership functions of the TSK controller

Table 2. Rules of the fuzzy critic

de/dt \ *e*	N	Z	P
N	*ZE* *l*=1	*PS* *l*=2	*PB* *l*=3
Z	*NS* *l*=4	*ZE* *l*=5	*PS* *l*=6
P	*NB* *l*=7	*NS* *l*=8	*ZE* *l*=9

The Gaussian and Sigmoid membership function were used in the first layer of TSK controller, which represents the negative μ_n, zero μ_z, and positive μ_p input values to the controller, and are expressed as follows: (see Fig. 7)

$$\mu_n = (1+\exp(10\upsilon+0.1))^{-1} \tag{19a}$$

$$\mu_z = \exp(-0.5\upsilon^2 / 0.1^2) \tag{19b}$$

$$\mu_p = (1+\exp(-10\upsilon+0.1))^{-1} \tag{19c}$$

where υ can be the error e or the derivative error de/dt of the x and y outputs of the milling process. The parameters selected based on the simple manual setting. The shapes of the membership functions (19) are designed based on expert knowledge and regulated by a simple trial and error on final responses of the plant.
Finally, the learning element would regulate the a_i, b_i and c_i parameters of the TSK according to the learning rule of Eqs. (17).

5. Sliding Mode Control (SMC)

Sliding mode control is one of the general methods for robust controlling of nonlinear systems. In this method, by defining a stable sliding surface s the trajectory reaches the manifold $s = 0$ in a limited time. By using the Taylor series, the time-delay terms of the displacements are approximated as follows:

$$\begin{aligned} \Delta x &= x(t) - x(t-\tau) \approx \tau \frac{dx}{dt} = \tau \dot{x} \\ \Delta y &= y(t) - y(t-\tau) \approx \tau \frac{dy}{dt} = \tau \dot{y} \end{aligned} \tag{20}$$

Therefore, the approximated forces in Eq. (8) are calculated as follows:

$$\begin{aligned} f_x &= -\frac{N}{2\pi}\left\{\alpha_1(\tau\dot{x})^3 + \beta_1(\tau\dot{y})^3 + \alpha_2(\tau\dot{x})^2 + \beta_2(\tau\dot{y})^2 + \alpha_3(\tau\dot{x}) + \beta_3(\tau\dot{y}) + 3\gamma_1(\tau\dot{x})^2(\tau\dot{y}) + 3\gamma_2(\tau\dot{x})(\tau\dot{y})^2 + 2\gamma_3(\tau\dot{x})(\tau\dot{y}) + \gamma_4\right\} \\ f_y &= \frac{N}{2\pi}\left\{\alpha_1'(\tau\dot{x})^3 + \beta_1'(\tau\dot{y})^3 + \alpha_2'(\tau\dot{x})^2 + \beta_2'(\tau\dot{y})^2 + \alpha_3'(\tau\dot{x}) + \beta_3'(\tau\dot{y}) + 3\gamma_1'(\tau\dot{x})^2(\tau\dot{y}) + 3\gamma_2'(\tau\dot{x})(\tau\dot{y})^2 + 2\gamma_3'(\tau\dot{x})(\tau\dot{y}) + \gamma_4'\right\} \end{aligned} \tag{21}$$

where f_i is an approximation of the cutting force F_i, and the same as before (see Eq. (7)), the $\hat{f}_i$ would be equal to f_i / m_i, (i=x,y). This problem is a regulation problem with $x_d = \dot{x}_d = \ddot{x}_d = 0$ and $y_d = \dot{y}_d = \ddot{y}_d = 0$. By considering two sliding surfaces as $S = [s_1 \quad s_2]^T$, we can define [32]:

$$\begin{aligned} s_1 &= \dot{x} + \rho_1 x \\ s_2 &= \dot{y} + \rho_2 y \end{aligned} \tag{22}$$

where ρ_2, $\rho_1 > 0$ are constants. The Lyapunov function is considered as follows:

$$V = \frac{1}{2}S^T S = \frac{1}{2}(s_1^2 + s_2^2) \tag{23}$$

and its derivative is as follows:

$$\begin{aligned} \dot{V} &= s_1\dot{s}_1 + s_2\dot{s}_2 = s_1\left[-2(\hat{\mu}_x + \hat{\mu}_{xp})\dot{x} - \omega_x^2 x - \hat{\delta}_1 x^2 - \hat{\delta}_2 x^3 + \hat{f}_x + u_x + \rho_1\dot{x}\right] + s_2\left[-2(\hat{\mu}_y + \hat{\mu}_{yp})\dot{y} - \omega_y^2 y - \hat{\lambda}_1 y^2\right. \\ &\left. - \hat{\lambda}_2 y^3 + \hat{f}_y + u_y + \rho_2\dot{y}\right] \le -k_{p1}s_1^2 - k_{p2}s_2^2 - \eta_1|s_1| - \eta_2|s_2| < 0 \qquad \eta_1, \eta_2 > 0 \end{aligned} \tag{24}$$

where k_{p1}, k_{p1}, η_1, and η_2 are the four positive constants. To reduce the output chatter and to increase the convergence rate, we considered the reaching law approach which involves a constant plus proportional decrease rate [33], as follows:

$$\begin{aligned} u_x &= u_{x_{eq}} - \beta_1 sign(s_1) - k_p s_1 \qquad u_{x_{eq}} = 2(\hat{\mu}_x + \hat{\mu}_{xp})\dot{x} + \omega_x^2 x + \hat{\delta}_1 x^2 + \hat{\delta}_2 x^3 - \hat{f}_x - \rho_1\dot{x} \\ u_y &= u_{y_{eq}} - \beta_2 sign(s_2) - k_p s_2 \qquad u_{y_{eq}} = 2(\hat{\mu}_y + \hat{\mu}_{yp})\dot{y} + \omega_y^2 y + \hat{\lambda}_1 y^2 + \hat{\lambda}_2 y^3 - \hat{f}_y - \rho_2\dot{y} \end{aligned} \tag{25}$$

It is also necessary to estimate the system time delay approximation as an uncertainty in the model parameters. It would make it feasible to apply the SMC to the original milling process by the following constraints.

$$\beta_1 \ge \eta_1 + \left|\hat{F}_x - \hat{f}_x\right| \quad , \quad \beta_2 \ge \eta_2 + \left|\hat{F}_y - \hat{f}_y\right| \tag{26}$$

6. Results

The values of the model and controller parameters are given in Table 1 and Table 3, while the initial conditions are assumed as $x(0) = -0.001mm$ and $\dot{x}(0) = \dot{y}(0) = y(0) = 0$. The parameters of controllers and logic function are based on a simple manual tuning, in order to both controllers present their best performances. The simulation result for ELIC and SMC can be summarized as follows.

Table 3. Parameters values of the proposed controllers

ELIC	Learning rate: η=1000		
SMC	k_{p1}= k_{p2}=0.1	ρ_1= ρ_2=50	β_1= β_2=0.1

Fig. 8 shows the behavior of the uncontrolled milling process. This time-delay system would be unstable within a concise time (about 0.07 s), and the amplitude of the vibrations goes to infinite in both directions.

Fig. 9 Compares x and y outputs time responses of the milling process in the presence of two different controllers SMC and ELIC. As it can be seen, the maximum overshoot for the ELIC is about 0.08 *mm*, while this value is 0.18 *mm* for the SMC. The settling time for ELIC is less than the SMC. However, the number of overshoots by the SMC is lower than the ELIC.

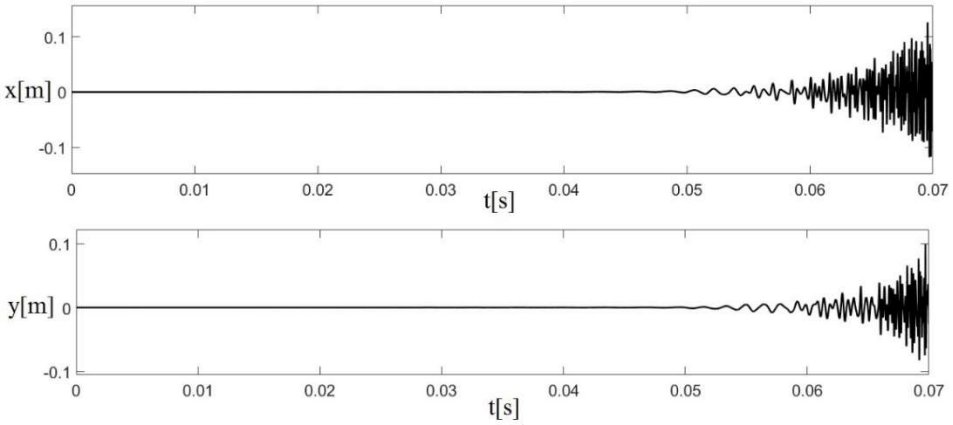

Fig. 8. Unstable behavior of the uncontrolled milling system

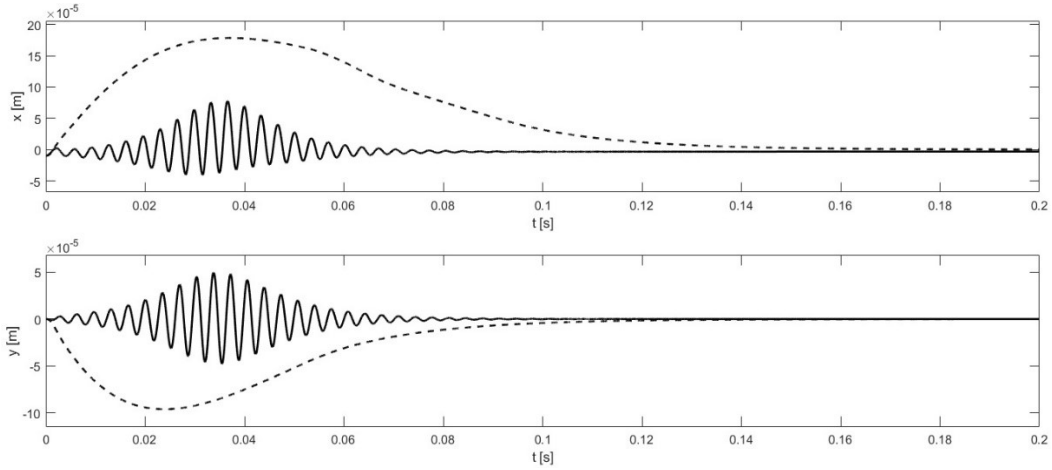

Fig. 9. *x* and *y* output time responses of the milling process using two different controllers (Dashed-line: SMC, Solid-line: ELIC)

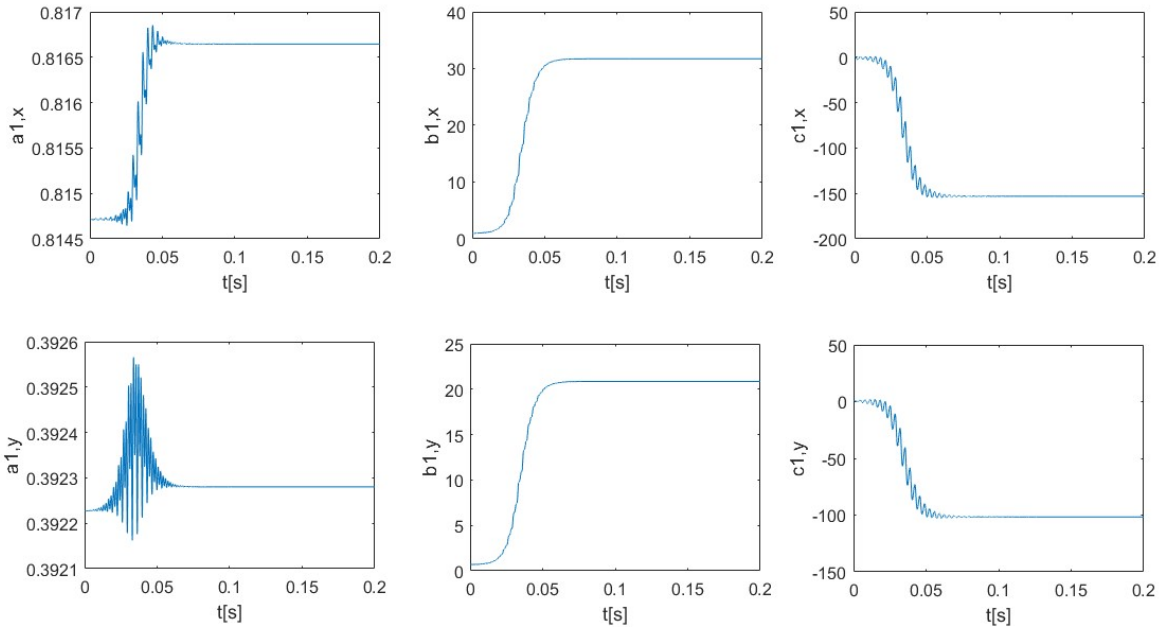

Fig. 10. Convergence behavior of the first elements of fuzzy neural network weights with random initial values; a_1, x, b_1, x, and c_1, x for the x-direction TSK and a_1, y, b_1, y, and c_1, y for the y-direction TSK (other elements show similar behavior)

Fig. 10 shows the convergence of a_1, b_1 and c_1 weights in the fourth layer of the TSK over the time. Other weights also have the same behaviour. All weights are converged from an initial random value to a stable value in about 0.05 *s*.
Fig. 11 compares the control efforts between the SMC and the ELIC. The maximum overshoot is about 1.4KN (*x*-direction) and 6.2KN (*y*-direction) for ELIC and SMC, respectively.
Fig. 12 compares the outputs time responses of 20%- parametric uncertainty in cutting forces F_x and F_y (see Eq. (8)) with different controllers. This uncertainty in the cutting forces may be due to the inappropriate modeling of the machines or replacement of the milling machine with another one. In the ELIC case, the weights of the TSK are firstly regulated for the nominal plant; then the same weights are applied to the plant with uncertainty up to 20% in cutting forces. This Figure reveals that both controllers are stable and robust. However, the SMC has a very larger amplitude in transient vibration.

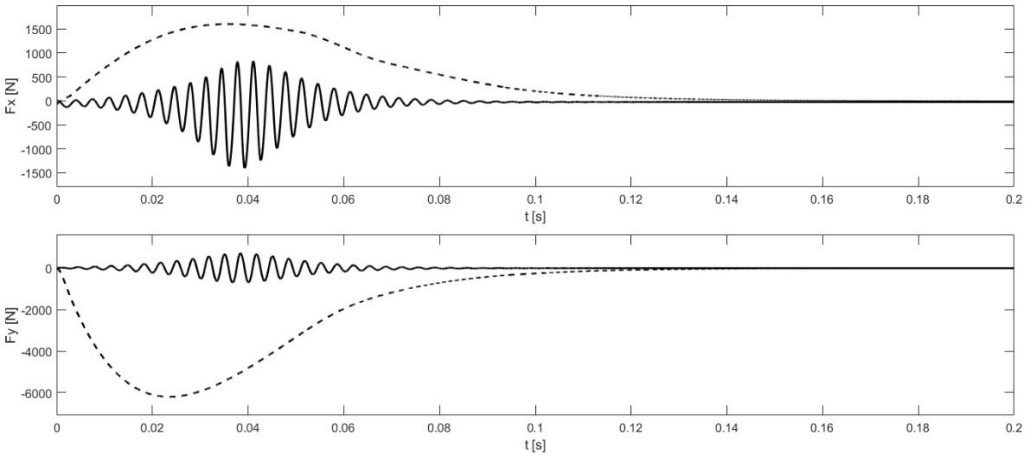

Fig. 11. Control efforts applied to the milling process by two different controllers (Dashed-line: SMC, Solid-line: ELIC)

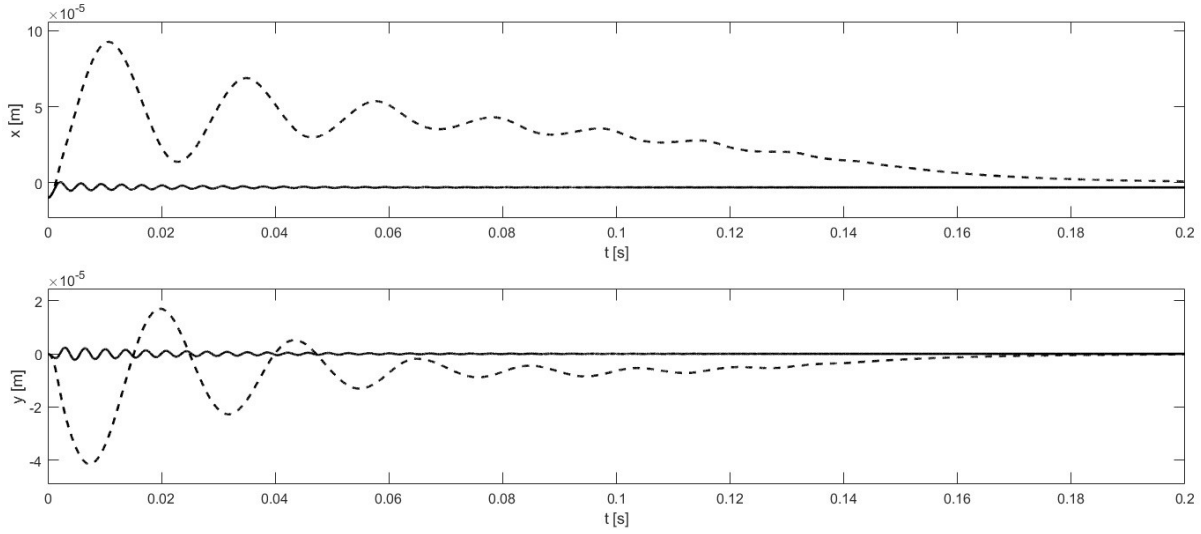

Fig. 12. The outputs time responses of the milling process with 20%- parametric uncertainty on cutting forces *Fx* and *Fy* with different controllers (Dashed-line: SMC, Solid-line: ELIC)

Finally, for the numerical evaluation of the performances between the two controllers, the Integral Absolute Error (IAE) and Integral of Time multiplied Square Error (ITSE) indicators are defined as follows

$$IAE = \int_0^\infty |e(t)|\, dt \tag{27a}$$

$$ITSE = \int_0^\infty t\,|e(t)|^2\, dt \tag{27b}$$

Table 4 compares the IAE and ITSE indicators for the nominal plant (Fig. 9), while Table 5 compares these indicators with an uncertain plant (Fig. 12) between the SMC and the ELIC. These two tables show a noticeable improvement in the performance of the milling process by ELIC.

Table 4. IAE and ITSE performance indices for ELIC and SMC controllers for the nominal plant (Fig. 9)

Controller/index	IAE		ITSE	
	y	x	y	x
ELIC	9.633e-7	1.601e-6	8.262e-13	1.57e-12
SMC	4.641e-6	1.195e-5	9.379e-12	6.802e-11
Improvement by ELIC	79%	86%	91%	97%

Table 5. IAE and ITSE performance indices for ELIC and SMC controllers with an uncertain plant (Fig. 12)

Controller/index	IAE		ITSE	
	y	x	y	x
ELIC	4.083e-8	5.658e-7	5.367e-16	1.599e-13
SMC	1.359e-6	5.583e-6	6.079e-13	1.182e-11
Improvement by ELIC	97%	89%	99%	98%

7. Discussion

In this paper, the milling process is considered as a MIMO strongly coupled nonlinear plant with time delay terms in cutting forces, where the high-speed aspects of the process were highlighted with a large value for spindle speed Ω and the large axial depth of cut ac of process (see Table 1). The spindle speed tool is selected a high value (10000 rpm) and the large axial depth of cut (22 mm). The frequency of the output vibrations is about 600 Hz at t=0.07s (see Fig. 8). To control such a high-frequency plant, one has to reduce time sampling for weight updates in ELIC. This problem was compensated in SMC by adding a term of proportional rate to the reaching law for increasing the speed of time responses.

In General, the ELIC control and identifies the plant dynamics simultaneously, while in the SMC one need to extract the control law from the mathematical model of the plant (Eq. (25)). Furthermore, when the identification and control are executing simultaneously, the convergence of outputs are increasing dramatically (see Fig. 10). These abilities would improve the robustness and generalization of the ELIC controllers in such complex MIMO plants with coupled dynamics. The current actuators used in the industry such as piezoelectric acts based on the current status of the plant outputs and their derivatives. One of the prominent advantages of the ELIC is the self-capturing of the complex nonlinear dynamics of cubic time-delays in the milling process, while SMC was forced to use the Taylor series approximation for delay terms (see Eq. (20)).

In ELIC, unlike all the other controllers, we design the critic instead of the controller. Since the duty of the critic is an evaluation of the whole system (plant plus controller), there is no need for the precise design of the critic, too. Thus, the fuzzy critic can be easily designed by a general sense of the desired operation of the whole system.

One of the shortcomings of the ELIC is the number of overshoots by the SMC which is lower than the ELIC (see Fig. 9). The main cause of this behavior is arising from the learning process in ELIC, where the initial TSK weights were selected randomly. In contrast, in the SMC the control law was designed and fixed for the process from the beginning. On the other hand, the milling process is a high-frequency plant; thus the sampling time in ELIC should be selected very low, while in SMC the proportional term in control law (see Eq. (25)) would compensate this requirement automatically. This phenomenon would apply a constraint on choosing the fast sensors and actuators in the practical implementation of the ELIC.

8. Conclusion

The MIMO milling process has been modelled using a nonlinear model with complete polynomials of order three for cutting forces functions. Comparison of the results of an intelligent control system named ELIC as a new application in the manufacturing field, with a well-known nonlinear robust strategy SMC showed both controllers can successfully stabilize the unstable plant. By selecting other initial conditions in displacements and velocities, it was realized that both controllers were able to stabilize the nominal plant and the plant with parametric uncertainty in cutting forces. The magnitude of the overshoot by ELIC was lower than the SMC. However, the number of overshoots by the SMC was lower than the ELIC, arising from the learning process in ELIC, where the initial weights were selected randomly. The considered milling process was a high-frequency plant. However, the ELIC could successfully control the outputs even in parametric uncertainty case. The IAE and ITSE performance indicators were more desirable in ELIC in both nominal and especially in uncertain plants. The advantages of the ELIC are simultaneous control and identification of the plant, continuous learning, high learning speed, good convergence, and robustness. Experimental validation to practical implementation in milling and theoretical proof of stability for ELIC will be considered as future work.

Conflict of Interest

The authors declared no potential conflicts of interest with respect to the research, authorship and publication of this article.

Funding

The authors received no financial support for the research, authorship and publication of this article.

References

[1] Kalpakjian, S., Schmid, S., *Manufacturing Processes for Engineering Materials*, 5th Edition, Agenda, 2014.
[2] Tobias, S., Fishwick, W., Theory of regenerative machine tool chatter. *The Engineer*, 205(7), 1958, 199-203.
[3] Tlusty, J., The stability of machine tools against self-excited vibrations in machining. *International Research in Production Engineering*, 1963, 465-474.
[4] Altintas, Y., Budak, E., Analytical Prediction of Stability Lobes in Milling. *CIRP Annals*, 44(1), 1995, 357-362.
[5] Moradi, H., Movahhedy, M.R., Vossoughi, G., Dynamics of regenerative chatter and internal resonance in milling process with structural and cutting force nonlinearities. *Journal of Sound and Vibration*, 331(16), 2012, 3844-3865.
[6] Moradi, H., Vossoughi, G., Movahhedy, M.R., Bifurcation analysis of nonlinear milling process with tool wear and process damping: sub-harmonic resonance under regenerative chatter. *International Journal of Mechanical Sciences*, 85, 2014, 1-19.
[7] Liu, K., Rouch, K., Optimal passive vibration control of cutting process stability in milling. *Journal of Materials Processing Technology*, 28(1-2), 1991, 285-294.
[8] Moradi, H., Bakhtiari-Nejad, F., Movahhedy, M., Tuneable vibration absorber design to suppress vibrations: an application in boring manufacturing process. *Journal of Sound and Vibration*, 318(1-2), 2008, 93-108.
[9] Rashid, A., Nicolescu, C.M., Design and implementation of tuned viscoelastic dampers for vibration control in milling. *International Journal of Machine Tools and Manufacture*, 48(9), 2008, 1036-1053.
[10] Hajikolaei, K.H., et al., Spindle speed variation and adaptive force regulation to suppress regenerative chatter in the turning process. *Journal of Manufacturing Processes*, 12(2), 2010, 106-115.
[11] Tsai, N.-C., Chen, D.-C., Lee, R.-M., Chatter prevention for milling process by acoustic signal feedback. *International Journal of Advanced Manufacturing Technology*, 47(9-12), 2010, 1013-1021.
[12] Elbestawi, M., Sagherian, R., Parameter adaptive control in peripheral milling. *International Journal of Machine Tools and Manufacture*, 27(3), 1987, 399-414.
[13] Huang, T., et al., Robust Active Chatter Control in Milling Processes With Variable Pitch Cutters. *Journal of Manufacturing Science and Engineering*, 140(10), 2018, 101005-1-9.
[14] Moradi, H., et al., Suppression of nonlinear regenerative chatter in milling process via robust optimal control. *Journal of Process Control*, 23(5), 2013, 631-648.
[15] Shin, Y., Vishnupad, P., Neuro-fuzzy control of complex manufacturing processes. *International Journal of Production Research*, 34(12), 1996, 3291-3309.
[16] Liu, Y., Zuo, L., Wang, C., Intelligent adaptive control in milling processes. *International Journal of Computer Integrated Manufacturing*, 12(5), 1999, 453-460.
[17] Janabi-Sharifi, F., A neuro-fuzzy system for looper tension control in rolling mills. *Control Engineering Practice*, 13(1), 2005, 1-13.
[18] Zuperl, U., Cus, F., Milfelner, M., Fuzzy control strategy for an adaptive force control in end-milling. *Journal of Materials Processing Technology*, 164, 2005, 1472-1478.
[19] Thellaputta, G.R., et al., Adaptive neuro fuzzy model development for prediction of cutting forces in milling with rotary tools. *Materials Today: Proceedings*, 5(2), 2018, 7429-7436.
[20] Sallese, L., et al., Intelligent fixtures for active chatter control in milling. *Procedia CIRP*, 55, 2016, 176-181.
[21] Ge, S.S., Tee, K.P., Approximation-based control of nonlinear MIMO time-delay systems. *Automatica*, 43(1), 2007, 31-43.
[22] Moradi, H., Movahhedy, M.R., Vossoughi, G.R., Robust control strategy for suppression of regenerative chatter in turning. *Journal of Manufacturing Processes*, 11(2), 2009, 55-65.
[23] Faassen, R., et al., Prediction of regenerative chatter by modelling and analysis of high-speed milling. *International Journal of Machine Tools and Manufacture*, 43(14), 2003, 1437-1446.
[24] Faassen, R., *Chatter prediction and control for high-speed milling*. Eindhoven: Eindhoven University of Technology, 2007.
[25] Farhangi, R., Boroushaki, M., Hosseini, S.H., Load–frequency control of interconnected power system using emotional learning-based intelligent controller. *International Journal of Electrical Power & Energy Systems*, 36(1), 2012, 76-83.
[26] Fakhrazari, A., Boroushaki, M., Adaptive critic-based neurofuzzy controller for the steam generator water level. *IEEE Transactions on Nuclear Science*, 55(3), 2008, 1678-1685.
[27] Khadem, S., et al., Design and implementation of an emotional learning controller for force control of a robotic laparoscopic instrument. *Frontiers in Biomedical Technologies*, 1(3), 2015, 168-181.
[28] Fatourechi, M., Lucas, C., Khakisedigh, A., *Control effort reduction using emotional learning*. in Proceedings of the Ninth Iranian Conference on Electrical Engineering, 2001.
[29] Barto, A.G., Sutton, R.S., Anderson, C.W., Neuronlike adaptive elements that can solve difficult learning control problems. *IEEE Transactions on Systems, Man, and Cybernetics*, 1983(5), 834-846.
[30] Berenji, H.R., Khedkar, P., Learning and tuning fuzzy logic controllers through reinforcements. *IEEE Transactions on Neural Networks*, 3(5), 1992, 724-740.
[31] Sugeno, M., Fuzzy identification of systems and its applications to modeling and control. *IEEE Transactions on Systems, Man, and Cybernetics*, 1985(1), 116-132.
[32] Slotine, J.-J.E., Li, W., *Applied nonlinear control*. Vol. 199, Prentice hall Englewood Cliffs, NJ, 1991.
[33] Gao, W., Hung, J.C., Variable structure control of nonlinear systems: A new approach. I*EEE Transactions on Industrial*

Electronics, 40(1), 1993, 45-55.

ORCID iD

Arash Bahari Kordabad https://orcid.org/0000-0001-8931-5372
Mehrdad Boroushaki https://orcid.org/0000-0001-8757-9219